International Journal of Biological Macromolecules xxx (xxxx) 148002

Contents lists available at ScienceDirect

International Journal of Biological Macromolecules

journal homepage: www.elsevier.com/locate/ijbiomac

Optimization and characterization of microbial transglutaminase production from *Streptomyces fradiae* and its usage in the dairy industry and medical applications

Fatemeh Merajian [a], Ahmad Asoodeh [a, b, *]

[a] Department of Chemistry, Faculty of Science, Ferdowsi University of Mashhad, Mashhad, Iran
[b] Cellular and Molecular Research Group, Institute of Biotechnology, Ferdowsi University of Mashhad, Mashhad, Iran

ARTICLE INFO

Keywords:
Microbial transglutaminase
Streptomyces fradiae
enzyme characterization
syneresis
blood clotting
histology

ABSTRACT

In this study, a non genetically modified strain of *Streptomyces fradiae* was cultured on ISP medium No. 4 medium supplemented with 1 % glycerol, casein, peptone, and yeast extract, and incubated at pH 7.2 and 27 °C for 7 days. Microbial transglutaminase (MTG) was purified using Q-Sepharose chromatography, and its molecular weight was determined to be 35.6 kDa via sodium dodecyl sulfate-polyacrylamide gel electrophoresis (SDS-PAGE). The purified MTG exhibited optimal activity at pH 8.5 and 50 °C. The enzyme's half-life was 88.12 ± 0.32 min at 30 °C and 49 ± 0.8 min at 50 °C. Additionally, the K_m and V_{max} values of the MTG reaction were 0.74 μM and 100.5 U/mg, respectively. The addition of 1 % MTG to the yogurt production process significantly reduced the pH from 4.8 to 4.5. Furthermore, syneresis decreased from 2.8 % to 1.5 %, indicating an improvement in the structure and quality of the treated yogurt. The isolated MTG significantly reduced blood clotting time in vitro from 457 ± 2 to 265 ± 2.5 s. In vivo, enzyme application led to a significant reduction in hemostasis time and blood loss in liver tissue. Moreover, histological observations revealed reduced liver damage and hemorrhage after 7 days. Overall, this study first reports that MTG from *S. fradiae* exhibits great potential as a biocatalyst in both the dairy industry and medical applications.

1. Introduction

Transglutaminases are intracellular and extracellular enzymes that play a significant role in catalyzing cross-linking between protein molecules [1]. Transglutaminase is a well-studied enzyme with a single polypeptide chain and a defined catalytic core. Its crystal structure, determined through X-ray crystallography, reveals features such as an N-terminal β-barrel domain and a catalytic triad consisting of cysteine, histidine, and aspartic acid [2]. These structural elements are vital for catalyzing protein cross-linking via transamidation reactions [3,4]. Transglutaminases are widely used in industrial processes to enhance physical properties such as strength, viscosity, elasticity, and water-holding capacity in various products [1].

MTG has diverse applications in the food industry [5]. In the meat industry, it improves the texture and juiciness of restructured beef and pork [2,6]. The texture of yogurt is primarily governed by production methods, with protein and emulsified fat enhancing gel strength and firmness. Rising demand for low-fat yogurt has prompted conventional improvements via non-fat solids and stabilizers, though regulatory limitations have shifted focus toward enzymatic alternatives [7]. Transglutaminase (TGase), which catalyzes an acyl transfer reaction between γ-carboxyamide groups of peptide-bound glutamine residues (acyl donor) and the primary amino groups of glutamine and lysine residues, has emerged as a promising agent for enhancing yogurt's structural and functional properties [8]. In dairy products, MTG enhances properties such as syneresis reduction in skimmed yogurt and modifies milk proteins, influencing hydration, rheology, and emulsification [9]. In bakery products, it enhances water-holding capacity, gluten strength during mixing and fermentation, and pasting behavior during cooking. However, excessive use of MTG should be avoided due to its potential association with celiac disease [5]. Additionally, MTG has gained interest in improving the stability, foaming properties, and emulsification potential of vegetable proteins, such as soybeans and faba beans [2,10].

Blood clotting, or hemostasis, is crucial for preventing excessive bleeding. It involves the formation of a platelet plug and a fibrin clot at the site of injury. Fibrin, derived from fibrinogen through the action of thrombin, plays a key role in clot formation. Recent research has highlighted the use of MTG to convert fibrinogen into fibrin, thereby facili-

* Corresponding author at: Cellular and Molecular Research Group, Institute of Biotechnology, Ferdowsi University of Mashhad, Mashhad, Iran.
E-mail address: Asoodeh@um.ac.ir (A. Asoodeh).

https://doi.org/10.1016/j.ijbiomac.2025.148002
Received 27 July 2025; Received in revised form 25 September 2025; Accepted 29 September 2025
0141-8130/

tating clot formation [11]. The application of MTG enhances the hemostatic properties of thrombin through cross-linking gelation [11]. In vitro experiments demonstrated a significantly reduced clotting time compared to traditional thrombin-based agents, indicating the potential of this approach for promoting faster hemostasis [12,13].

MTG has been isolated from *Bacillus nakamurai* and a variant of *Bacillus subtilis* [14], *Streptoverticillium S-8112* [15], *Bacillus subtilis* spores [16], and *Streptomyces mobaraensis* [17]. These studies provide valuable insights into the isolation and purification of MTG from different microbial sources. Actinobacteria, particularly actinomycetes, are prolific producers of bioactive secondary metabolites, including antibiotics, anticancer agents, immunosuppressants, and enzymes. Marine actinomycetes, especially the genus Streptomyces, are commercially valuable due to their widespread distribution and capacity to generate novel compounds. Nutritional sources and environmental factors significantly influence metabolite production, prompting optimization of culture conditions for *S. fradiae* to enhance antimicrobial yields [18].

The aim of the study was to investigate the ability of MTG enzyme production from *S. fradiae* and to investigate the efficacy of the extracted enzyme in improving the properties of yogurt and blood homeostasis, and in reducing liver damage in a mouse model.

The present study is the first report of MTG purification and biochemical characterization from *S. fradiae*. The effect of MTG on syneresis and the quality of yogurt was examined. Moreover, the impact of the enzyme on blood clotting time was investigated under in vitro and in vivo conditions. Histological analyses on liver damage and hemorrhage were carried out by hematoxylin-eosin (HE) staining.

2. Materials and methods

The strain of *S. fradiae* (ATCC10745) was obtained from the Persian Type Culture Collection (Iran). The Q-Sepharose resin was procured from GE Healthcare (USA). N-α-carbobenzoxyl-glutaminyl-glycine (N-CBZ-Gln-Gly) and L-glutamic acid γ-monohydroxamate (LGH) and gelatin (type A from porcine) were acquired from Sigma-Aldrich (USA). Culture media were purchased from Merck (Germany). Other chemicals and reagents were sourced from Sigma (USA), and BALB/c mice were supplied by the Faculty of Pharmacy, Mashhad, Iran.

2.1. Microbial culture

S. fradiae, an Actinobacteria species, was cultivated under controlled laboratory conditions. Specifically, the microorganisms were grown on a solid agar medium known as Inorganic Salt Starch Agar (ISP Medium No. 4) [19] ISP medium No. 4 was formulated with specific chemical components, including 10 g/L soluble starch, 1 g/L dipotassium phosphate, 1 g/L sodium chloride, 1 g/L magnesium sulfate heptahydrate, 2 g/L calcium carbonate, 2 g/L ammonium sulfate, 0.001 g/L manganous chloride heptahydrate, 0.001 g/L zinc sulfate heptahydrate, and 0.001 g/L ferrous sulfate heptahydrate [20] with a pH of 7.2 [14,21]. The microbial culture was conducted at a temperature of 27 °C for seven days [17]. Finally, to support the growth and maintenance of the microorganism during enzyme production, the ISP medium No. 4 was supplemented with glycerol (1 %), casein (1 %), peptone (1 %), and yeast extract (1 %) [22–24].

2.2. Enzyme assay

The activity of MTG was demonstrated by evaluating the formation of hydroxamate with a specific substrate, N-CBZ-Gln-Gly [25]. A 1.0 mL substrate solution was prepared by mixing 0.2 mL of 0.1 M hydroxylamine, 0.4 mL of 0.2 M Tris-HCl buffer (pH 6.0), 0.2 mL of 0.01 M reduced glutathione, and 0.2 mL of 0.15 M substrate. To assay enzyme activity, 1 mL of the substrate solution was mixed with 0.4 mL of the enzyme solution and incubated at 37 °C for 10 min, followed by quenching the reaction by adding 133 μL of 12 % HCl, 133 μL of 12 % trichloroacetic acid (TCA), and 133 μL of 5 % ferric trichloride solution in 0.1 M HCl [14]. After centrifugation at 10,000 RPM for 5 min, the supernatant's absorbance was analyzed at 525 nm [26]. L-glutamic acid γ-monohydroxamate was used for calibration. One unit of transglutaminase is defined as the amount of enzyme that produces 1.0 μmol of L-glutamic acid γ-monohydroxamate per minute at 37 °C [1,14].

2.3. Screening of transglutaminase production

Qualitative screening of the colonies was initially performed using the filter paper disc method (FPD) [27]. The FPD assay was based on a hydroxamate assay utilizing hydroxylamine and CBZ-Gln-Gly as specific substrates for MTG for MTG from *S. fradiae*, which is reported for the first time. The FPD assay placed colonies of *S. fradiae* on an ISP medium No. 4 agar plate, and 30 μL of the substrate solution (containing 37.5 mM substrate, 12.5 mM glutathione, and 125 mM hydroxylamine dissolved in 200 mM citrate buffer with pH 6.0) was loaded onto the disc and maintained at 37 °C for 240 min. After that, 10 μL of 5 % $FeCl_3$ in 15 % TCA was loaded onto the FPD and kept at the previous temperature for 1 h. The resulting color change was observed [28]. The color intensity of the FPDs was evaluated using ImageJ software. A red-burgundy color generation indicated the formation of the hydroxamate-ferric complex [1,23]. Quantitative screening of activity was evaluated by enzyme assay, which involves measuring the formation of *Z*-glutamyl-hydroxamate-glycine, producing a detectable iron (III) colored complex at 525 nm [1,29].

2.4. Preliminary optimization using the one-factor-at-a-time (OFAT) approach

The cultivation parameters were optimized using One-Factor-at-a-Time (OFAT) protocols to achieve maximal MTG production. The experiment used ISP medium No. 4 as the base control medium. Different parameters, including ten different temperatures ranging from 20 °C to 70 °C (with increments of 5 degrees) [14], types of nitrogen and carbon sources, pH in the range of 3.0 to 9.5 (with increments of 0.5 units) [14], and inoculum concentration varying from 0.5 % to 3 % (*v*/v), were examined independently. A suspension of bacterial cells of 1.5×10^8 CFU/mL (equivalent to 0.5 of the McFarland standard) was chosen for the inoculation process [23].

2.5. MTG purification

After optimization, the bacterial culture was centrifuged for 10 min at 10,000 RPM. Next, ammonium sulfate was added to 100 mL of crude extract to reach 85 % (*w*/*v*) saturation [26]. After 24 h of incubation at 4 °C, the precipitate was collected by centrifugation at 10,000 RPM for 20 min. The sediment was dissolved in 20 mM Tris buffer (pH 8.0) and then dialyzed for 24 h.

To isolate MTG, Q-Sepharose chromatography was used. The column was equilibrated with 20 mM Tris buffer (pH 8.0), and the dialyzed sample was subsequently loaded at 4 °C. In the following stage, the column was washed with NaCl in Tris buffer, with the NaCl concentration varying from 0.1 to 0.5 M.

To determine protein concentration, a Bradford assay was conducted using bovine serum albumin (BSA) as the standard. The collected fractions were analyzed using SDS-PAGE, employing a 12 % separating gel [17]. A sample buffer (10 μL) was mixed with 40 μL of protein, heated in boiling water for 5 min, and loaded onto the gel. The gel was stained with Coomassie Brilliant Blue R-250 (Jin et al., 2016). The molecular weight of MTG was estimated using a Vivantis protein ladder (California, USA).

2.6. Influence of pH and temperature on the activity and stability of S. fradiae MTG

To investigate the impact of pH on MTG activity, various buffers were utilized: 50 mM acetate buffer (pH 3.0–5.5), 50 mM sodium phosphate buffer (pH 5.5–8.0), and 50 mM Tris-HCl buffer (pH 8.0–9.5) [26]. To assess the enzyme's stability under different pH levels, samples were incubated in the buffers mentioned above for 1 h at 4 °C, followed by an enzymatic activity evaluation under optimal conditions.

Furthermore, the purified MTG was exposed to varying temperatures (20 °C–70 °C) while being incubated with a substrate [26]. To analyze the residual activity of incubated MTG, CBZ was used as a substrate. The enzyme's thermal stability was evaluated by incubating it at different temperatures for 1 h, followed by an activity assessment under optimal buffer and temperature conditions [30].

2.7. Impact of metal ions on MTG activity

MTG activity was assessed under various ionic conditions. The influence of the ions Na^+, K^+, Ni^{2+}, Ca^{2+}, Mg^{2+}, Zn^{2+}, Ba^{2+}, Mn^{2+}, Cu^{2+}, Fe^{3+}, Hg^{2+}, Co^{2+}, and Pb^{2+} was measured at concentrations of 2 mM and 5 mM. The purified MTG was placed in separate solutions containing 500 μL of each sample and incubated for 1 h under optimal conditions [26]. Enzyme activity under these ionic conditions was compared to that observed in a control solution devoid of ions [26].

2.8. Impact of chemical agents, organic solvents, and chemical detergents on MTG activity

The impact of chemical agents on MTG activity was examined. Specifically, dinitrothiocyanobenzene (DNTB), ethylenediaminetetraacetic acid (EDTA), NaN_3, beta-mercaptoethanol (β-ME), dithiothreitol (DTT), 1,10-phenanthroline, sodium dodecyl sulfate (SDS), phenylmethylsulfonyl fluoride (PMSF), cetyltrimethyl ammonium bromide (CTAB), and Triton X-100 were evaluated at concentrations of 2 mM and 5 mM [17,31].

Furthermore, the impact of ethanol, hexane, butanol, methanol, glycerol, acetone, dimethyl sulfoxide (DMSO), propanol, and ethyl acetate was independently assessed on MTG. The enzyme was incubated at 10 % and 20 % under optimal conditions for 1 h. Additionally, the effect of chemical cleansing agents on MTG activity was investigated. The enzyme activity of a test lacking additives or reagents (i.e., the control) was considered 100 %. The remaining activity of MTG was determined under control conditions [31,32].

2.9. Evaluation of the kinetic parameters of MTG

The effect of different concentrations of SGZ (ranging from 0.25 to 10 μM) on MTG activity was investigated [31]. To determine the kinetic parameters K_m and V_{max}, a Michaelis-Menten curve was constructed using GraphPad Prism 8 software. Moreover, the thermal stability of *S. fradiae* MTG was evaluated by estimating its half-life at varying temperatures of 30 °C and 50 °C [14].

2.10. The impact of purified MTG on dairy texture

MTG plays a significant role in enhancing the quality and sensory attributes of yogurt by facilitating protein cross-linking [33]. In this study, fresh low-fat cow's milk (1.5 %) was divided into control and experimental groups, with the latter receiving a 1 % (*w/v*) addition of MTG. Both groups underwent heating at 85 °C for 30 min, followed by cooling to 45 °C before the introduction of a 2 % (w/v) yogurt starter culture. The samples were incubated at 42 °C for 4 h. Afterwards, they were stored at 4 °C for 12 h [34]. Subsequent evaluations focused on physicochemical and sensory characteristics, including pH and syneresis.

2.10.1. Syneresis

The syneresis percentage of yogurt, a key quality indicator, can be measured using a centrifugation method. The most common approach to observe syneresis is the centrifugation method [35]. In this process, a specific weight of yogurt is centrifuged at 3000 rpm and 4 °C for 5 min, allowing the separation of components [36]. The free water (serum) that rises above the yogurt layer is then measured. The syneresis percentage is calculated using the formula:

$$\text{Synthesis}\% = \frac{\text{Weight of supernatant (g)}}{\text{Weight of yogurt sample (g)}} \times 100\%$$

2.11. Effect of S. fradiae MTG on in-vitro blood clotting

Fresh human blood was used for the assay. Blood samples were procured and dispensed into test tubes. The samples were randomized into three distinct groups: Group A (600 μL blood, no additional substances), Group B (500 μL blood, supplemented with 100 μL normal saline), and Group C (500 μL blood, supplemented with 100 μL MTG). Following randomization, clotting time was determined by assessing the absence of blood flow after inverting the test tubes. The resulting clots were carefully extracted, excess liquid was absorbed using filter paper, and the clots were weighed [12]. Concurrently, alterations in volume for both clots and plasma were meticulously determined. To elucidate the impact of the enzyme on red blood cells (RBCs) and clot formation, the samples were promptly examined under a microscope after adding reagents.

2.12. Hemostatic agent

Gelatin was dissolved at 25 % *w*/w in PBS buffer (pH 7.4) and maintained at 65 °C until use. To ensure optimal performance, the gelatin was utilized immediately after preparation. MTG powder was dissolved in pre-cooled PBS (pH 7.4) and kept on ice until use. The hemostatic agent was prepared by mixing the warm gelatin (65 °C) and MTG solutions in a 2:1 volume ratio immediately before application [13].

2.12.1. Effect of S. fradiae MTG on in-vivo blood clotting

In this study, 36 female Balb/c mice (weighing 18–23 g) were divided into three groups of 12 animals: a blank control group, a gelatin group, and a gelatin-MTG mix group, to evaluate the hemostatic efficacy in the liver as the anatomical site.

The mice were anesthetized during the operation via an intraperitoneal injection of ketamine and xylazine hydrochloride (2.5:1.5) [37]. For liver hemostasis surgery, an abdominal midline incision was made to expose the liver following local disinfection. A sterile gauze was placed under the liver to facilitate the procedure. A 0.5 cm-long, 0.3 cm-deep sagittal incision was made in the lobe of the mice's liver using a scalpel. The liver incision was observed for approximately 10 s to confirm the successful preparation of the blood model. Subsequently, a gelatin-MTG mixture (or gelatin solution containing 2.4 U/mg) (≈60 μL) was applied immediately after removing the accumulated blood. Mice in the control group received no treatment. Total blood loss was determined by measuring the weight of sterile gauze before and after surgery [13].

At 0, 3, and 7 days post-surgery, the mice were euthanized via carbon dioxide inhalation. The hemostatic treatment area and adjacent tissues were excised and fixed in a 4 % paraformaldehyde solution (pH 7.0) for a minimum of 24 h. Subsequently, the samples underwent dehydration using graded alcohols and dimethylbenzene, followed by paraffin embedding [37]. Tissue sections of 5 μm thickness were then prepared and stained with hematoxylin-eosin (HE) for histological and pathological examination [13].

2.13. Statistical analyses

Statistical analyses were conducted using three replicates, and the average data were graphed using Prism 8 software for visualization. The results are presented as mean values ± standard deviations, and statistical significance was evaluated using one-way analysis of variance (ANOVA).

3. Results

3.1. Bacterial cultivation and MTG production

MTG is found both inside and outside of bacterial cells and is expressed by a wide range of bacteria. In the current study, for the first time, the production of MTG in *S. fradiae* was induced by cultivating the bacterium in ISP medium No. 4 supplemented with glycerol, casein, peptone, and yeast extract. The cultured strain of *S. fradiae* formed sticky colonies that produced MTG.

To investigate the growth pattern of *S. fradiae* on ISP medium No. 4, the culture was incubated at 27 ˚C for 7 days. The results showed that the exponential phase of the bacterium began 96 h after inoculation and persisted for 24 h. Subsequently, the stationary phase started after 120 h, followed by the death phase at 192 h (Fig. 1). Moreover, based on MTG activity, the maximum MTG production was achieved under optimized conditions of pH 7.2, a temperature of 27 ˚C, and an inoculation volume of 1.5 % (*V*/V) (Fig. 2a). Additionally, the presence of glycerol, peptone, yeast extract, and casein in the culture medium enhanced enzyme activity (Fig. 2b).

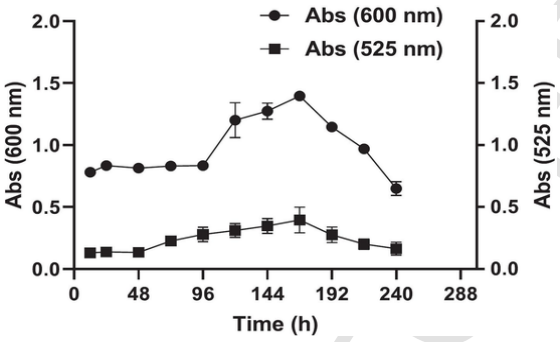

Fig. 1. The bacterial culture of *S. fradiae* displaying the growth curve over time and the enzymatic activity of MTG. The maximum MTG activity was observed at 168 h of inoculation.

3.2. Screening of MTG-producing streptomyces

In this study, qualitative screening was conducted on *S. fradiae* to assess its capacity for transglutaminase production. The screening results revealed that the isolate exhibited MTG activity, as evidenced by a discernible color change in the filter paper discs (FPDs) to a red-burgundy color (Fig. 3). The color intensity of the FPDs was also evaluated using ImageJ software, and the color intensity of Disc A was 165.5, and Disc B was 142.6.

3.3. Purification of MTG

The purification process of MTG was carried out through ammonium sulfate precipitation (85 %), followed by dialysis and Q-Sepharose chromatography (Table 1). All fractions were collected, and their absorbances were read at 280 nm, and enzyme activity was determined at 525 nm. Fraction 0.3, exhibiting the highest enzyme activity and protein absorbance, was selected for further analyses. The specific activity of MTG in the cell-free supernatant was 0.51 ± 0.2 U/mg and increased to 2.40 ± 1.0 U/mg after ion-exchange chromatography (Fig. 4a). In this study, the molecular weight of the purified MTG was determined to be 35.6 kDa by SDS-PAGE gel electrophoresis (Fig. 4b).

3.4. Impact of pH and temperature on MTG activity and stability

MTG exhibited activity across a wide pH range, with the highest activity at pH 8.5 (Fig. 5a). The activity of *S. fradiae* MTG was temperature-dependent, with optimal activity observed at 50 ˚C. Beyond the optimal temperature, a reduction in MTG activity was observed (Fig. 5b). Notably, the enzyme demonstrated remarkable stability, with approximately 90 % residual activity maintained at temperatures of 45 ˚C and 55 ˚C, and optimal stability (100 %) observed at 50 ˚C.

3.5. Impact of metal ions, chemical agents, solvents, and chemical detergents on MTG activity

Our findings demonstrated that various metal ions impacted the activity of MTG. Specifically, Na^{+}, Ca^{2+}, Mg^{2+}, Zn^{2+}, Mn^{2+}, Cu^{2+},

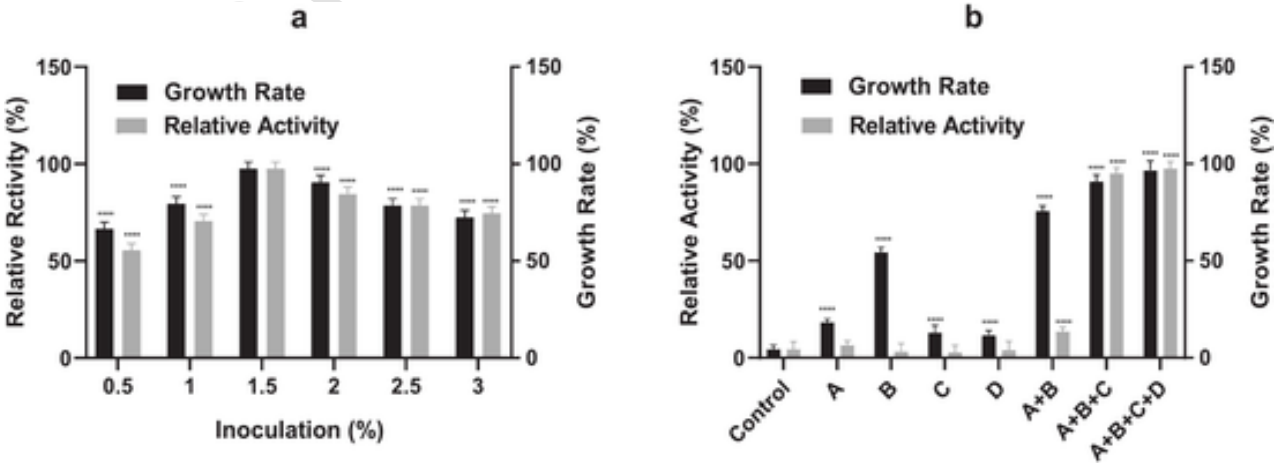

Fig. 2. Optimization of MTG production. a) Percentage of inoculation and its effect on the growth rate of bacteria and relative activity of MTG. b) The ISP medium No. 4 (control) was additionally supplemented with A (glycerol (1 %)), B (casein (1 %)), C (yeast extract (1 %)), and D (peptone (1 %)). *: $P < 0.05$, **: $P < 0.01$, ***: $P < 0.001$, and ****: $P < 0.0001$ compared to control and 1.5 % by two-way ANOVA.

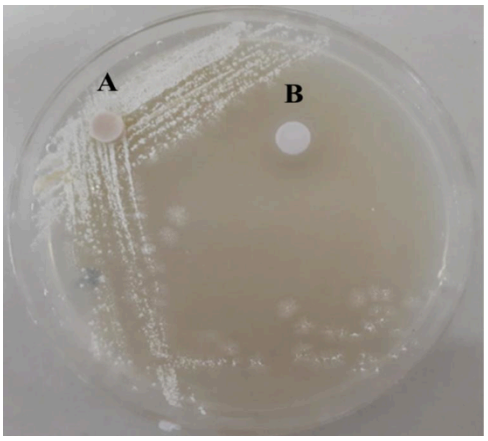

Fig. 3. FPD assay of colonies on the ISP medium No. 4 agar plate. FPD loaded on *S. fradiae*'s colonies (A) shows red-burgundy color, while (B) shows no color changes. (For interpretation of the references to color in this figure legend, the reader is referred to the web version of this article.)

Co^{2+}, and Pb^{2+} were found to enhance MTG activity, as depicted in Fig. 6a. On the other hand, DNTB strongly inhibited MTG activity by 40 % at a concentration of 5 mM. In comparison, MTG inhibition of 20 % was observed at a concentration of 5 mM EDTA, as shown in Fig. 6b. Methanol, ethanol, and butanol at concentrations of 10 % and 20 % were found to increase MTG activity compared to the control, as demonstrated in Fig. 6c. Among these solvents, methanol exhibited the most robust enhancement of MTG activity. Additionally, the presence of SDS at a concentration of 2 mM increased MTG activity (Fig. 6d), indicating its positive effect on enzyme activity.

3.6. Kinetic parameters

The half-life of MTG was determined to be 88.12 ± 0.32 min and 48.75 min at 30 °C and 50 °C, respectively (Fig. 7a). Additionally, based on the Michaelis-Menten curve, the Km, V_{max}, and K_{cat} of MTG were calculated as 17.26 ± 0.7 mg/mL, 20.82 ± 0.3 mU/mg, and 61.23 ± 0.6 ± 0.6 S^{-1}, respectively (Fig. 7b). These findings provide insights into the stability and enzymatic characteristics of MTG under different temperature conditions and substrate concentrations.

3.7. The effect of MTG on dairy texture

The addition of 1 % MTG during yogurt production significantly influenced its physicochemical properties. MTG reduced the pH from 4.8 to 4.5. Additionally, the enzyme decreased syneresis from 2.8 % to 1.5 % compared to the control group (Fig. 8).

3.8. Effect of isolated MTG on in-vitro blood clotting

The time required for the blood to stop flowing was considered clotting time and was conducted by inverting the blood samples. The clotting time was 457 ± 2 s for group A (control) and increased to 726 ± 2 s for group B (normal saline). Notably, the clotting time of group C (MTG) was shortened and reached 265 ± 2.5 s (Table 2). The weight of the clots represents the disparity between the total clot weight and the weight of the added reagents. The mean clot weight in group A and group B was 0.247 ± 0.01 g and 0.202 ± 0.07 g, respectively, while it was 0.273 ± 0.21 g in group C, which was noticeably heavier than the control group (Table 2).

Observations of the shape and volume of the clots and plasma revealed that, upon clotting, there was no bleeding flow upon immediate inversion of the test tubes (see Fig. 9a). The volume of clots in group C (MTG) was larger than in groups A and B (Fig. 9b). The final volume of residual plasma is presented in Table 2. Furthermore, tactile examina-

Table 1
Purification steps of microbial transglutaminase from *S. fradiae*.

Purification steps	Activity (U/ml)	Protein (mg/ml)	Specific activity (units/mg)	Total protein (mg)	Total activity (unit)	Purification (fold)	Yield (%)
Culture medium	0.29	0.57	0.51	142.00	72.42	1.00	100.00
Ammonium sulfate precipitation	0.23	0.34	0.68	14.77	10.04	1.33	7.07
Q-Sepharose	0.12	0.05	2.4	0.53	1.27	4.70	1.75

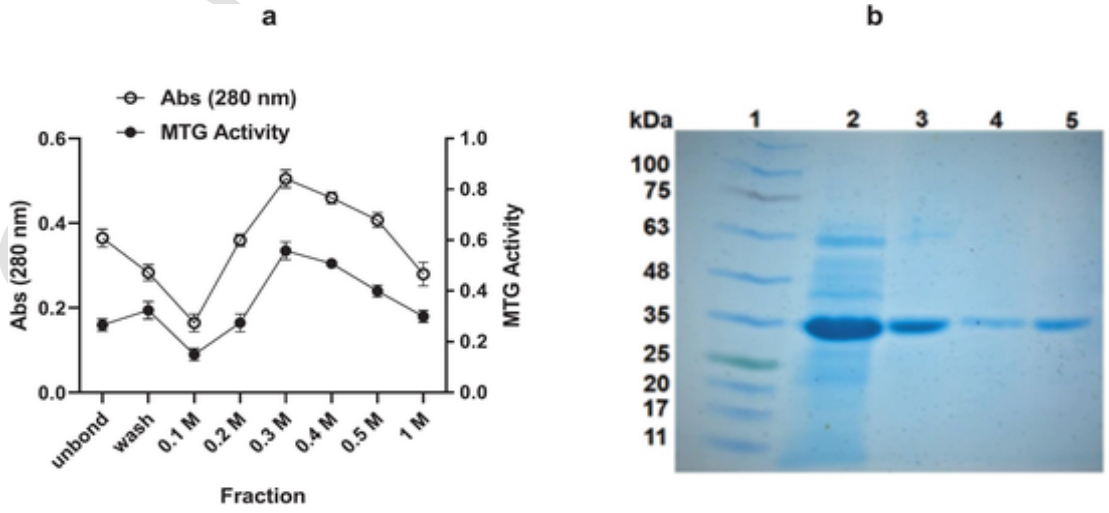

Fig. 4. a) Q-Sepharose fractionation of MTG. b) SDS-PAGE analysis. 1: protein ladder, 2: crude MTG, 3: fraction 0.3 M of the chromatography, 4: fraction 0.4 M of the chromatography, 5: fraction 0.5 M of the chromatography.

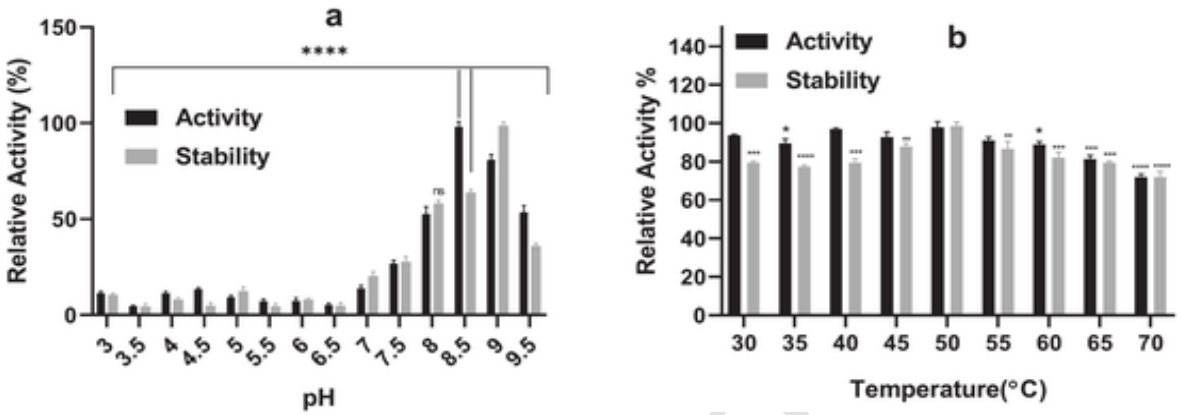

Fig. 5. The effects of pH (a) and temperature (b) on MTG activity and stability. Maximum activity was considered 100 % activity. *: $P < 0.05$, **: $P < 0.01$, ***: $P < 0.001$, and ****: $P < 0.0001$ compared to pH 8.5 and temperature of 50 °C by two-way ANOVA.

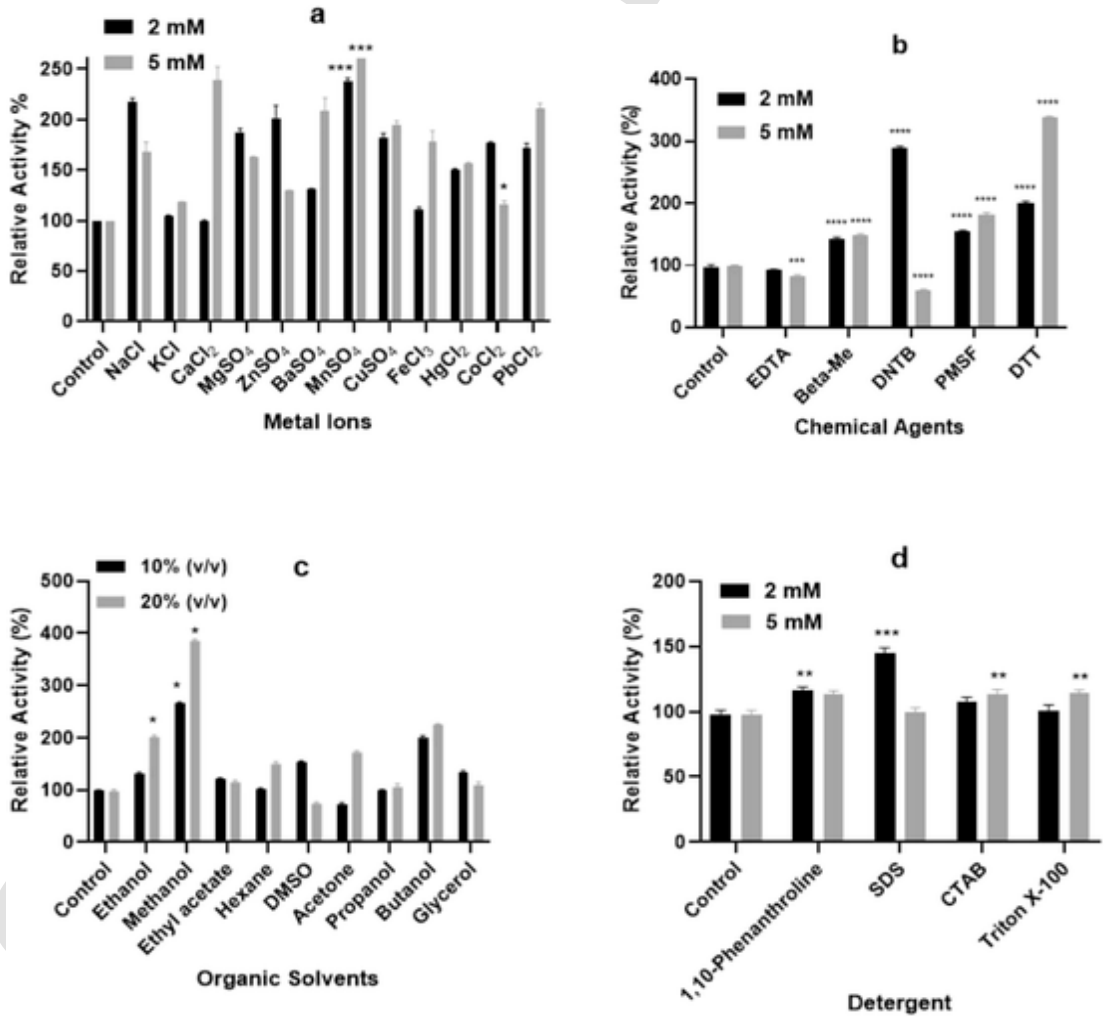

Fig. 6. Influences of various additives on the enzyme activity. a) Effects of metallic ions on MTG activity. b) The effects of chemical agents on enzymatic activity. c) Effects of organic solvents and d) Chemical detergents on MTG activity. Enzyme activity was considered 100 % for the control. *: $P < 0.05$, **: $P < 0.01$, ***: $P < 0.001$, and ****: $P < 0.0001$ compared to control by two-way ANOVA.

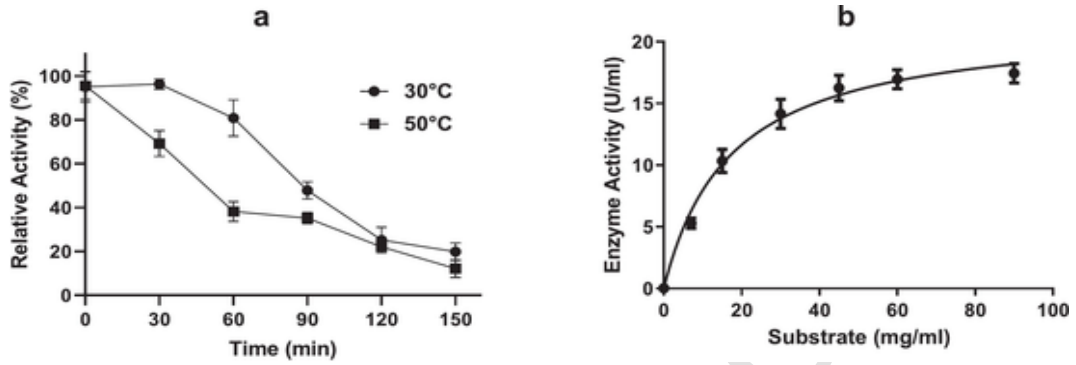

Fig. 7. The profile of residual activity of MTG over time at 30 °C and 50 °C. a) Enzymatic activity of *S. fradiae* MTG. b) Michaelis-Menten diagram. K_m and V_{max} of MTG toward CBZ were 17.26 ± 0.7 mg/ml and 20.82 ± 0.3 U/mL, respectively.

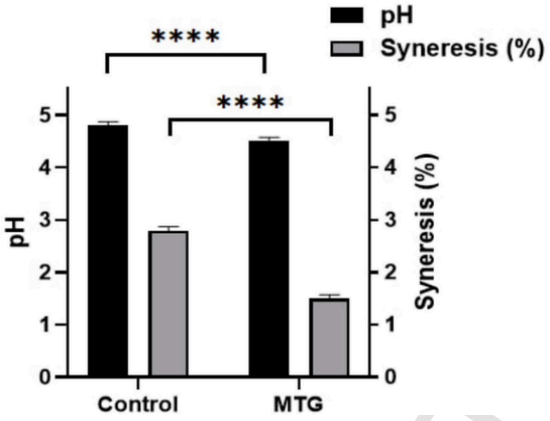

Fig. 8. Characteristics of yogurt. Effect of MTG addition to yogurt on pH and syneresis compared to control (****: $P < 0.0001$).

Table 2
Comparison of clotting time and weight of the clots between groups A, B, and C. **: $P < 0.01$ and ***: $P < 0.001$ compared to group A by two-way ANOVA.

Group	V_0 (μL)	Weight of clot (g)	Volume of plasma (μL)	Clotting time (s)
A (blood)	600	0.247 ± 1	242 ± 1.5	457 ± 2
B (blood + normal saline)	600	0.202 ± 0.07	250 ± 1**	726 ± 2***
C (blood + MTG)	600	0.273 ± 0.21	240 ± 1.3	265 ± 2.5***

tion revealed that the clots in group C exhibited more elasticity and strength (Fig. 9b). Microscopic examination demonstrated that group A exhibited standard agglutination of red blood cells (RBCs), group B displayed dispersed RBCs, and group C showed tightly agglutinated RBCs arranged closely without gaps, indicating the influence of MTG on blood clotting (Fig. 10).

3.9. Effect of isolated MTG on in-vivo blood clotting

To investigate the effect of isolated MTG on in-vivo blood clotting, hemostasis time, blood loss, and histological analysis were performed.

3.9.1. Hemostasis time

In the liver hemostasis model, the control group and the gelatin group exhibited persistent bleeding for 5.17 ± 0.025 min (Fig. 11a). In

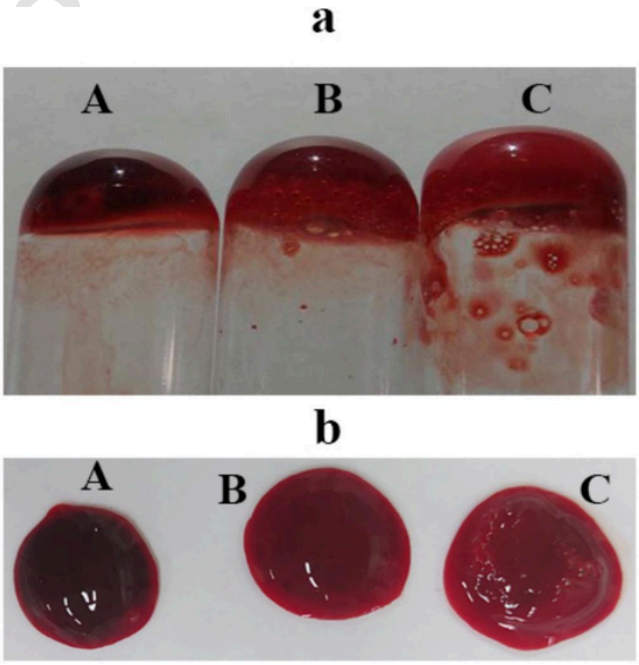

Fig. 9. The clotting effect of MTG in tubes (a) and slide (b) (A) blood (control), (B) blood + normal saline, and (C) blood + MTG.

contrast, the gelatin-MTG mixture group demonstrated 2.26 ± 0.045 min in bleeding time, approximately halving the duration (Fig. 11a).

3.9.2. Blood loss

Blood loss serves as a critical parameter in the evaluation of hemostatic efficacy. In the liver hemostasis model, the application of a gelatin-MTG mixture demonstrated a significant reduction reached to 0.1 ± 0.01 in blood loss compared to both the untreated control group and the gelatin group (0.27and 0.25 respectively), as illustrated in Fig. 11b. Furthermore, the average blood loss observed in the gelatin group was approximately equivalent to that of the untreated control group, as depicted in Fig. 11b.

Blood loss serves as a critical parameter in the evaluation of hemostatic efficacy. In the liver hemostasis model, the application of a gelatin-MTG mixture demonstrated a 1 ± 0.01 reduction in blood loss compared to both the untreated control group and the gelatin group, as illustrated in Fig. 11b. Furthermore, the average blood loss observed in

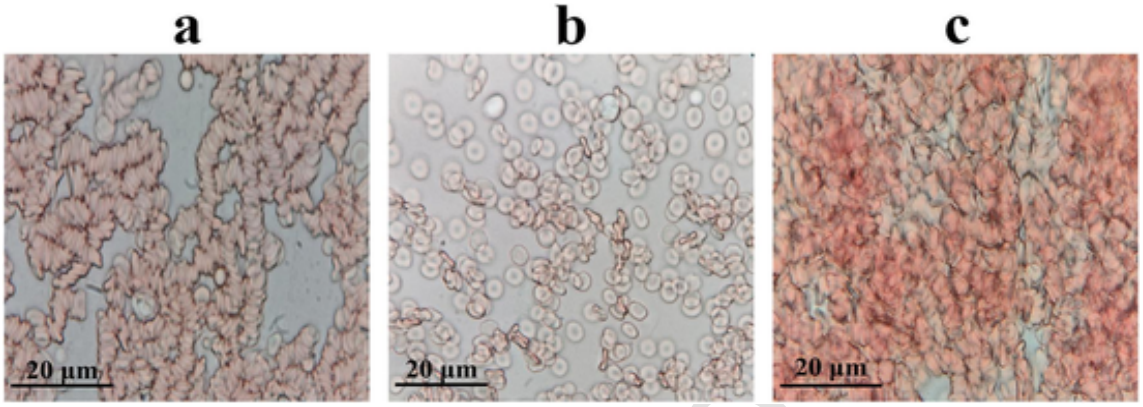

Fig. 10. Images (100×) are taken from slides prepared from (a) blood, (b) blood + normal saline, and (c) blood + MTG. The red globules are red blood cells. (For interpretation of the references to color in this figure legend, the reader is referred to the web version of this article.)

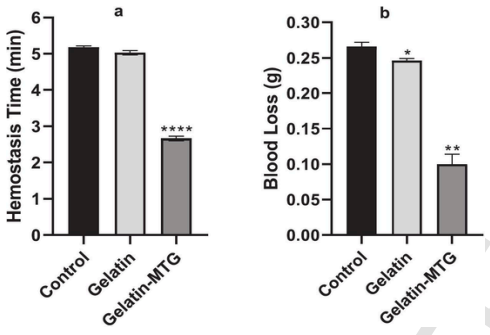

Fig. 11. Evaluation of hemostatic agent: a) Hemostasis time (min) and. b) Blood loss (g) in the liver hemostasis model. **: $P < 0.05$, **: $P < 0.01$, ***: $P < 0.001$, and ****: $P < 0.0001$.*

the gelatin group was approximately equivalent to that of the untreated control group, as depicted in Fig. 11b.

3.9.3. Histology analysis

The results of the microscopic evaluation of liver tissue demonstrate the significant effects of novel hemostatic agents, including gelatin and MTG, on hepatic injury caused by hemorrhage and necrosis. On day 0, the control group had severe vacuolar degeneration and extensive areas of coagulative necrosis in hepatocytes (Fig. 12). This condition is indicative of a critical response to hemorrhage-induced injury [38]. On day 3, in the gelatin group, microscopic evaluation showed that the bleeding area contained red blood cells and hepatic vascular congestion, with signs of vacuolar degeneration and coagulative necrosis similar to the control group, indicating rebleeding. However, the severity of inflammation in the gelatin group was less than that in the control group, indicating the initial protective effects of this agent (Fig. 12). On day 7, in the gelatin group, more signs of recovery were observed. Although there were still signs of injury, the infiltration of inflammatory cells was reduced, and the proliferation of fibroblasts increased. Meanwhile, the control group still showed severe liver injury and persistent inflammation. In particular, the gelatin-MTG group showed no signs of significant injury on day 7, and there were no red blood cells in this group (Fig. 12).

4. Discussion

Our study demonstrated that the bacterium's exponential growth phase began at 96 h post-inoculation, lasting 24 h, followed by stationary and death phases, while optimal MTG production was achieved at pH 7.2, 27 °C, and 1.5 % (*V*/V) inoculation volume, with glycerol, peptone, yeast extract, and casein enhancing enzymatic activity offering key insights for industrial enzyme production. Several studies have investigated the optimization of culture media for MTG production [22,24,31,39]. Various microbial sources, culture conditions, and nutrient composition can affect microbial growth and MTG production. Junqua et al. reported a specific activity of 0.14 U/mL for transglutaminase from *S. cinnamoneum* [22], whereas Cui et al. observed 7.6 U/mg for MTG from *S. hygroscopicus* [31], and Portilla-Rivera et al. recorded a maximum activity of 0.240 U/mL for transglutaminase [24].

The screening analyses confirmed MTG activity in the isolate, as indicated by a distinct red-burgundy color change in the FPDs. This color change results from the enzymatic cross-linking of CBZ-Gln-Gly with hydroxylamine and the formation of a colored complex, which serves as a reliable indicator of MTG activity. Bourneow et al. reported that MTGase-positive colonies were visually scored from 0 to 3 based on color intensity [40]. Other similar results from FPD assays have been reported for *Streptomyces* [41], actinomycetes [23], soil and wastewater bacteria [28,40,42]. These findings validate the isolate's potential as a novel MTG producer, aligning with previous studies on diverse microbial sources.

Three-step purification of MTG increased its specific activity from 0.51 ± 0.2 U/mg to 2.40 ± 1.0 U/mg, with SDS-PAGE confirming a molecular weight of 35.6 kDa for the purified enzyme. Various MTGs have been purified; for example, Yokoyama et al. reported a molecular weight of 35.6 kDa [43], Jin et al. determined a 37.8 kDa for MTG-TX [17], and Lu et al.reported a range of 39.5–40.1 kDa for transglutaminase [44], reflecting the enzyme's conserved structural characteristics.

MTG demonstrated broad pH activity, peaking at pH 8.5, and exhibited temperature-dependent activity, with optimal performance at 50 °C. The observed alkaline and thermal stability is important for potential industrial applications.

Duerasch et al. demonstrated that casein micelles disrupted under alkaline conditions (around pH 8.5 or higher) can be reassembled through the action of MTG. The alkaline treatment exposes internal casein fractions, such as α_s2-casein, making them more accessible for enzymatic cross-linking. As a result, the cross-linked micelles exhibited enhanced stability and modified physical characteristics, including changes in size and oligomerization [45]. Kieliszek et al. reported that certain dough or flour systems contain alkaline buffers, and the alkaline stability of TGase enables its effective functionality in such matrices, thereby enhancing dough strength, elasticity, and loaf volume. Moreover, post-baking or enzyme addition treatments may exhibit greater efficacy when the enzyme remains stable at elevated pH levels. Although general reviews of mTGase applications in bakery products pri-

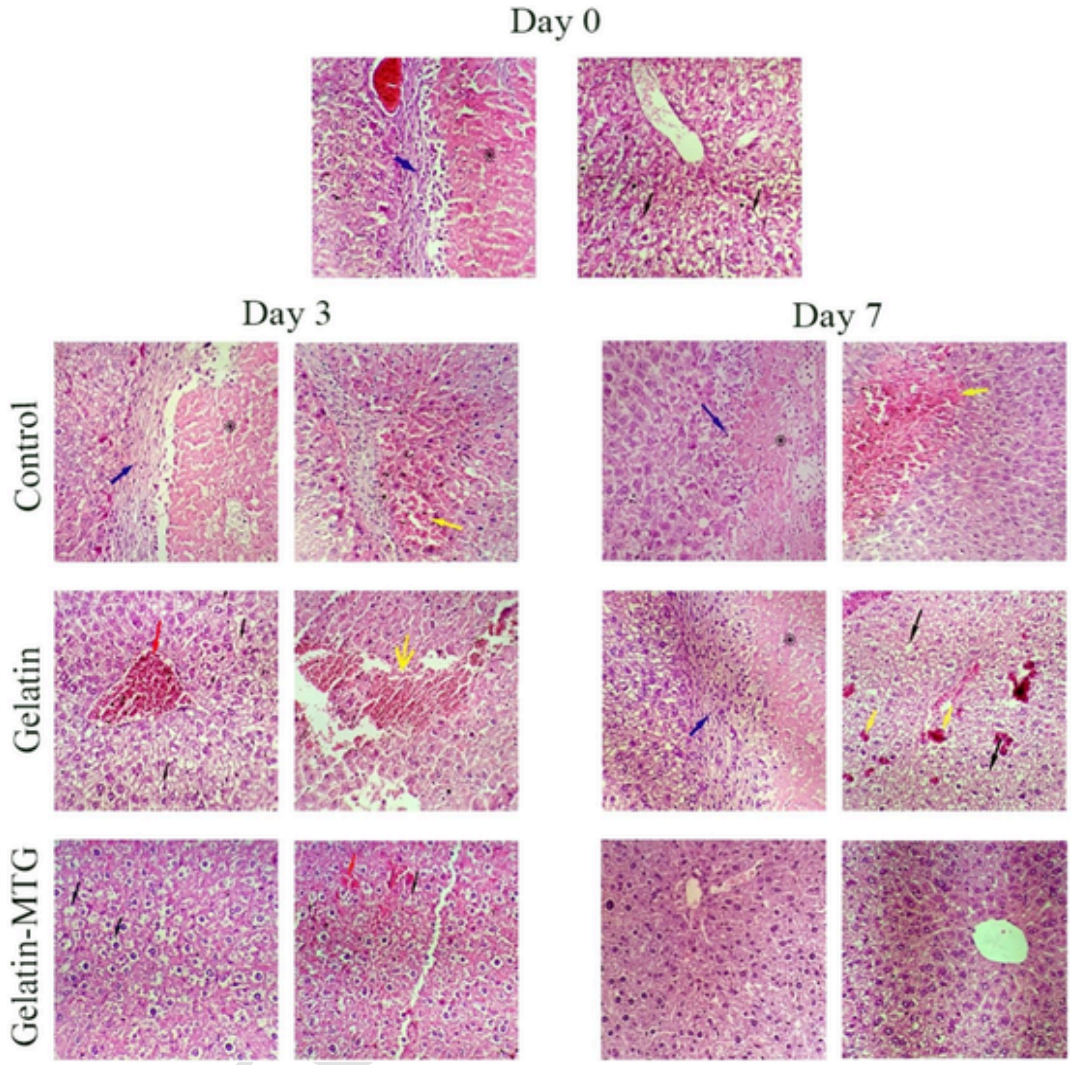

Fig. 12. Histological studies of hemostatic agents on the liver. Hematoxylin-eosin stained images of liver tissue treated with a mixture of gelatin-microbial transglutaminase enzyme and gelatin on days 0, 3, and 7 after surgery from two different areas (400×). Microscopic evaluation revealed hepatocyte vacuolar degeneration (black arrows), a large area of coagulative necrosis of hepatocytes (star), fibroblast proliferation and inflammatory cells infiltration around the necrotic area (blue arrow), hemorrhagic area including red blood cells (yellow arrow), and hepatic vascular congestion (red arrow). (For interpretation of the references to color in this figure legend, the reader is referred to the web version of this article.)

marily emphasize improvements in texture, volume, and related attributes under neutral to slightly acidic conditions, the enzyme's alkaline stability substantially broadens its potential applications and formulation options [46]. Other reported microbial transglutaminases had optimal activity between 20 °C and 50 °C and pH 5.0 to 7.0 [23,44]. Under slightly alkaline environments, the MTG enzyme possesses favorable ionization states of active site residues. Our results reflect MTG's enzymatic stability and adaptability, highlighting its potential for diverse industrial applications.

The current study revealed that metal ions such as Na^{+}, Ca^{2+}, Mg^{2+}, $Zn^{2}+$, Mn^{2+}, Cu^{2+}, Co^{2+}, and Pb^{2+} significantly enhanced MTG activity, while DNTB and EDTA inhibited it by 40 % and 20 %, respectively, at 5 mM concentrations. Moreover, organic solvents (methanol, ethanol, and butanol at concentrations of 10 %) and SDS at 2 mM positively influenced MTG activity and highlighted the enzyme's adaptability to diverse chemical environments. Ando et al. observed that Zn^{2+} and Cu^{2+} resulted in 85 % and 20 % enzyme inhibition, respectively [15]. However, other examined metal ions did not exhibit significant inhibition. Shi et al. revealed that the MTG enzyme exhibited potent inhibition in the presence of Fe^{3+}, Zn^{2+}, and Cu^{2+}, whereas the enzyme was not inhibited by Ca^{2+}, Mg^{2+}, and Ba^{2+} [26]. These last two reports were not consistent with our findings. MTG purified from *Bacillus subtilis* and *Streptoverticillium* species showed calcium-independent activity. In contrast, the enzymatic reaction catalyzed by transglutaminases in vertebrates and some invertebrates requires Ca^{2+} to expose a cysteine residue at the active site [30].

The enhancement of MTG activity by metal ions can be attributed to their roles in stabilizing the enzyme's structure and acting as cofactors, as demonstrated in studies on microbial transglutaminases [43,47]. Indeed, various metal ions have differential effects on structure and MTG activity. Inhibition by DNTB and EDTA likely results from the disruption of critical cysteine residues and chelation of essential metal ions, respectively [48]. The positive effects of organic solvents (methanol, ethanol, and butanol) and SDS may stem from their ability to modify the enzyme's microenvironment, enhancing substrate accessibility and stability, with methanol showing the most significant improvement due to its favorable interactions with the enzyme's active site [46]. These findings highlight MTG's adaptability to diverse chemical conditions, supporting its potential for industrial applications.

The half-life of MTG was determined to be 88 ± 0.32 min at 30 °C and 49 ± 0.8 min at 50 °C, while kinetic analysis revealed a K_m of 17.26 ± 0.7 mg/mL, a V_{max} of 20.82 ± 0.3 U/mL and a K_{cat} of 61.23 ± 0.6 s^{-1}, indicating its thermal stability and catalytic efficiency under varying conditions. Cui et al., through the hydroxamate procedure and analysis using a Lineweaver-Burk plot, demonstrated that the enzyme had a K_m value of 54.69 mM and a V_{max} value of 1.28 U/mL [31].

In research conducted by Jin et al., the K_m values of MTG-TX in the presence of N-α-CBZ-Gln-Gly and hydroxylamine hydrochloride were measured to be 23.12 mM and 1.37 mM, respectively. The V_{max} value of MTG-TX was determined to be 8.46 $U.mg^{-1}$, indicating the maximum rate of substrate conversion. Additionally, the K_{cat} value of MTG-TX, representing the turnover number, was calculated to be 1.83 s^{-1}, illustrating the enzyme's catalytic efficiency [17].

Sorde et al. reported K_m values of 33.92 mM and 121.42 mM for MTG extracted from *Bacillus nakamurai* (B4) and a variant of *Bacillus subtilis* (C2), respectively. In addition, the V_{max} values were measured to be 5.28 mM/min and 7.27 mM/min for B4 and C2, respectively [14].

The observed half-life of MTG, being longer at 30 °C (88 ± 0.32 min) than at 50 °C (49 ± 0.8 min), reflects its thermal stability, which is consistent with studies showing that microbial transglutaminases maintain structural integrity at moderate temperatures but degrade faster at higher temperatures due to denaturation. The kinetic parameters, including a K_m of 17.26 ± 0.7 mg/mL, V_{max} of 20.82 ± 0.3 U/mL, and K_{cat} of 61.23 ± 0.6 s^{-1}, indicate efficient substrate binding and catalytic turnover, aligning with findings that MTG exhibits high catalytic efficiency under optimized conditions.

The addition of 1 % MTG during yogurt production significantly improved its physicochemical properties, reducing pH from 4.8 to 4.5 and decreasing syneresis from 2.8 % to 1.5 %. Similar findings regarding the change of pH from 4.4 to 4.2 have been reported in previous studies [33].

García-Gómez et al. reported that the presence of MTG prevented the syneresis of low-fat yogurts [34].

The results can be attributed to MTG's ability to cross-link casein proteins, enhancing the yogurt matrix's stability and water-holding capacity. The reduction in syneresis from 2.8 % to 1.5 % aligns with findings that MTG strengthens protein networks, minimizing whey separation and improving texture. The slight decrease in pH from 4.8 to 4.5 may result from enhanced microbial activity or protein interactions, further contributing to yogurt's stability and quality. This research underscores the potential application of MTG in the dairy industry to enhance product quality.

The clotting time was significantly reduced to 265 ± 2.5 s in group C (MTG) compared to 457 ± 2 s in group A (control) and 726 ± 2 s in group B (normal saline), while the clot weight (0.273 ± 0.21 g) and volume in group C were notably higher, with clots exhibiting greater elasticity, strength, and tightly agglutinated RBCs.

The tightly agglutinated RBCs observed in group C align with findings that MTG promotes stronger intercellular interactions, improving clot elasticity and reducing bleeding. These results are consistent with studies showing that MTG accelerates clot formation and enhances clot quality by stabilizing fibrin networks, making it a promising agent for improving hemostasis [12,31,48]. These observations demonstrate that MTG could facilitate the cross-linking between amino acids in blood proteins, thereby promoting rapid clotting.

The gelatin-MTG mixture significantly reduced both hemostasis time and blood loss in the liver hemostasis model, halving the bleeding duration and demonstrating superior hemostatic efficacy compared to the control and gelatin-only groups. The significant reduction in hemostasis time and blood loss observed with the gelatin-MTG mixture can be attributed to MTG's ability to cross-link fibrin and other proteins, enhancing clot stability and mechanical strength, as demonstrated in studies on MTG's role in hemostasis [31,48]. Gelatin, when combined with MTG, forms a more robust and adhesive matrix, improving its ability to seal wounds and reduce bleeding, as shown in research on gelatin-based hemostatic agents [49]. These findings align with evidence that MTG enhances the efficacy of hemostatic materials by promoting stronger clot formation and tissue adhesion, and reduces blood loss, which is crucial in treating liver injuries with severe bleeding. This hemostatic action reduces the need for blood transfusions and minimizes additional tissue damage, leading to faster recovery.

Meanwhile, research in mouse models offers crucial proof-of-concept but has inherent limitations for human translation. Key differences in physiology, immune response, healing rates, cellular turnover, and genetics mean outcomes may not directly predict human results. Therefore, these findings are a vital first step that justifies further study in more complex, human-relevant systems.

Overall, the results of this study indicate the high potential of novel hemostatic agents in reducing liver injury and accelerating the healing process. These findings can form the basis for further research in the field of hemostatic therapies and their clinical applications in wound management and surgery.

In conclusion, this paper presents the isolation and purification of transglutaminase from a novel *S. fradiae* strain. The transglutaminase was successfully purified through three purification steps, resulting in a purified enzyme with a molecular mass of approximately 35.6 kDa. The enzymatic activity was optimal at pH 8.5 and a temperature of 50 °C. These findings indicate that the enzyme remains active under alkaline conditions and at high temperatures. The addition of MTG significantly decreased the acidity and lowered syneresis in enzyme-treated yogurts, which could be used in the dairy industry to enhance product quality. The addition of MTG promoted rapid clotting, improving clot elasticity and reducing bleeding. Moreover, the gelatin-MTG mixture significantly reduced both hemostasis time and blood loss in liver injury. Altogether, the characterized MTG derived from *S. fradiae* possesses remarkable features that could be considered as a promising candidate for developing innovative applications in the dairy industry and therapeutics, such as wound and surgical incisions. The potential for enzyme use in the treatment of chronic wounds (which have different conditions in terms of pH, biofilm formation, and the presence of proteases) requires further studies in this field.

CRediT authorship contribution statement

Fatemeh Merajian: Writing – original draft, Software, Investigation. **Ahmad Asoodeh:** Writing – review & editing, Validation, Supervision, Funding acquisition.

Ethical approval

No humans participated in the basis of this research. All procedures involving animals' protocol were conducted in accordance with the guidelines and the standards in the eighth edition of "Guide for the Care and Use of Laborator Animals. The Institutional Animal Ethics Committee of the Ferdowsi University of Mashhad approved the experimental protocol (Document no: IR.UM.REC.1401.053).

Funding

This study was funded by Iran National Science Foundation: INSF (Grant number: 4032699) and Ferdowsi University of Mashhad, Mashhad, Iran [Grant number: 3/52688, 1399/07/01].

Declaration of competing interest

Fatemeh Merajian declares that she has no conflict of interest. Ahmad Asoodeh declares that he has no conflict of interest.

Acknowledgments

The authors appreciate the support provided by the Research and Technology Council of Ferdowsi University of Mashhad, Mashhad, Iran (Grant number: 3/52688, 1399/07/01).

Data availability

The data from the current study will be made available upon request.

References

[1] L. Duarte, C.R. Matte, C.V. Bizarro, M.A.Z. Ayub, Transglutaminases: part I—origins, sources, and biotechnological characteristics, World J. Microbiol. Biotechnol. 36 (2020), https://doi.org/10.1007/s11274-019-2791-x.
[2] N. Miwa, Innovation in the food industry using microbial transglutaminase: keys to success and future prospects, Anal. Biochem. 597 (2020), https://doi.org/10.1016/j.ab.2020.113638.
[3] M. Te Yang, C.H. Chang, J.M. Wang, T.K. Wu, Y.K. Wang, C.Y. Chang, T.H.T. Li, Crystal structure and inhibition studies of transglutaminase from *Streptomyces mobaraense*, J. Biol. Chem. 286 (2011), https://doi.org/10.1074/jbc.M110.203315.
[4] T. Kashiwagi, K. ichi Yokoyama, K. Ishikawa, K. Ono, D. Ejima, H. Matsui, E. ichiro Suzuki, Crystal structure of microbial transglutaminase from *Streptoverticillium mobaraense*, J. Biol. Chem. 277 (2002), https://doi.org/10.1074/jbc.M203933200.
[5] V. Kolotylo, K. Piwowarek, M. Kieliszek, Microbiological transglutaminase: biotechnological application in the food industry, Open Life Sci 18 (2023), https://doi.org/10.1515/biol-2022-0737.
[6] S. Sorapukdee, P. Tangwatcharin, Quality of steak restructured from beef trimmings containing microbial transglutaminase and impacted by freezing and grading by fat level, Asian Australas. J. Anim. Sci. 31 (2018), https://doi.org/10.5713/ajas.17.0170.
[7] B. Ozer, H. Avni Kirmaci, S. Oztekin, A. Hayaloglu, M. Atamer, Incorporation of microbial transglutaminase into non-fat yogurt production, Int. Dairy J. 17 (2007), https://doi.org/10.1016/j.idairyj.2006.02.007.
[8] M. Ziarno, D. Zaręba, The effect of the addition of microbial transglutaminase before the fermentation process on the quality characteristics of three types of yogurt, Food Sci. Biotechnol. 29 (2020), https://doi.org/10.1007/s10068-019-00640-6.
[9] S.M. Taghi Gharibzahedi, M. Koubaa, F.J. Barba, R. Greiner, S. George, S. Roohinejad, Recent advances in the application of microbial transglutaminase crosslinking in cheese and ice cream products: a review, Int. J. Biol. Macromol. 107 (2018), https://doi.org/10.1016/j.ijbiomac.2017.10.115.
[10] H.S. Mostafa, Microbial transglutaminase: an overview of recent applications in food and packaging, Biocatal. Biotransformation 38 (2020) 161–177, https://doi.org/10.1080/10242422.2020.1720660.
[11] Y. Liu, D. Kopelman, L.Q. Wu, K. Hijji, I. Attar, O. Preiss-Bloom, G.F. Payne, Biomimetic sealant based on gelatin and microbial transglutaminase: an initial in vivo investigation, J. Biomed. Mater. Res. B Appl. Biomater. 91 (2009) 5–16, https://doi.org/10.1002/jbm.b.31368.
[12] T. Yu, Y. Guan, X. Xie, Y. Huang, J. Tang, Improved thrombin hemostat using the cross-linked gelatin by microbial transglutaminase, Int J Polym Sci 2015 (2015), https://doi.org/10.1155/2015/985286.
[13] F. Lv, X. Cong, W. Tang, Y. Han, Y. Tang, Y. Liu, L. Su, M. Liu, M. Jin, Z. Yi, Novel hemostatic agents based on gelatin-microbial transglutaminase mix, Sci. China Life Sci. 60 (2017), https://doi.org/10.1007/s11427-015-9019-x.
[14] K.L. Sorde, L. Ananthanarayan, Isolation, screening, and optimization of bacterial strains for novel transglutaminase production, Prep. Biochem. Biotechnol. 49 (2019), https://doi.org/10.1080/10826068.2018.1536986.
[15] H. Ando, M. Adachi, K. Umeda, A. Matsuura, M. Nonaka, R. Uchio, H. Tanaka, M. Motoki, Purification and characteristics of a novel transglutaminase derived from microorganisms, Agric. Biol. Chem. 53 (1989), https://doi.org/10.1271/bbb1961.53.2613.
[16] S. Suzuki, Y. Izawa, K. Kobayashi, Y. Eto, S. Yamanaka, K. Kubota, K. Yokozeki, Purification and characterization of novel transglutaminase from *bacillus subtilis* spores, Biosci. Biotechnol. Biochem. 64 (2000), https://doi.org/10.1271/bbb.64.2344.
[17] M. Jin, J. Huang, Z. Pei, J. Huang, H. Gao, Z. Chang, Purification and characterization of a high-salt-resistant microbial transglutaminase from Streptomyces mobaraensis, J. Mol. Catal. B: Enzym. 133 (2016), https://doi.org/10.1016/j.molcatb.2016.07.005.
[18] A. Paradkar, A. Trefzer, R. Chakraburtty, D. Stassi, Streptomyces genetics: a genomic perspective, Crit. Rev. Biotechnol. 23 (2003), https://doi.org/10.1080/713609296.
[19] Z. Khosravi Babadi, G. Ebrahimipour, J. Wink, A. Narmani, C. Risdian, Isolation and identification of Streptomyces sp. Act4Zk, a good producer of Staurosporine and some derivatives, Lett. Appl. Microbiol. 72 (2021), https://doi.org/10.1111/lam.13415.
[20] A. Vaezi-Kakhki, A. Asoodeh, Comparison of different methods for synthesis of iron oxide nanoparticles and investigation of their cellular properties, and antioxidant potential, Int. J. Pharm. 645 (2023), https://doi.org/10.1016/j.ijpharm.2023.123417.
[21] V. Incani, C. Danumah, Y. Boluk, Nanocomposites of nanocrystalline cellulose for enzyme immobilization, Cellulose 20 (2013), https://doi.org/10.1007/s10570-012-9805-2.
[22] M. Junqua, R. Duran, C. Gancet, P. Goulas, Optimization of microbial transglutaminase production using experimental designs, Appl. Microbiol. Biotechnol. 48 (1997), https://doi.org/10.1007/s002530051124.
[23] J.R. Xavier, K.V. Ramana, R.K. Sharma, Screening and statistical optimization of media ingredients for production of microbial transglutaminase, Def Life Sci J 2 (2017), https://doi.org/10.14429/dlsj.2.11369.
[24] O.M. Portilla-Rivera, S.J. Téllez-Luis, J.A.R. de León, M. Vázquez, Production of microbial transglutaminase on media made from sugar cane molasses and glycerol, Food Technol. Biotechnol. 47 (2009).
[25] N. Grossowicz, E. Wainfan, E. Borek, H. Waelsch, The enzymatic formation of hydroxamic acids from glutamine and asparagine, J. Biol. Chem. 187 (1950), https://doi.org/10.1016/s0021-9258(19)50936-x.
[26] Y.G. Shi, L. Qian, N. Zhang, C.R. Han, Y. Liu, Y.F. Zhang, Y.Q. Ma, Study on separation and purification of the transglutaminase, Appl. Mech. Mater. (2012), https://doi.org/10.4028/www.scientific.net/AMM.121-126.443.
[27] C. Bourneow, S. Benjakul, A. H-Kittikun, Hydroxamate-based colorimetric method for direct screening of transglutaminase-producing bacteria, World J. Microbiol. Biotechnol. 28 (2012), https://doi.org/10.1007/s11274-012-1017-2.
[28] J.E. Folk, P.W. Cole, Mechanism of action of guinea pig liver transglutaminase. I. Purification and properties of the enzyme: identification of a functional cysteine essential for activity, J. Biol. Chem. 241 (1966).
[29] L. Lorand, O.M. Lockridge, L.K. Campbell, R. Myhrman, J. Bruner-Lorand, Transamidating enzymes. II. A continuous fluorescent method suited for automating measurements of factor XIII in plasma, Anal. Biochem. 44 (1971), https://doi.org/10.1016/0003-2697(71)90363-0.
[30] S.J. Lin, Y.F. Hsieh, L.A. Lai, M.L. Chao, W.S. Chu, Characterization and large-scale production of recombinant Streptoverticillium platensis transglutaminase, J. Ind. Microbiol. Biotechnol. 35 (2008), https://doi.org/10.1007/s10295-008-0373-2.
[31] L. Cui, G. Du, D. Zhang, H. Liu, J. Chen, Purification and characterization of transglutaminase from a newly isolated Streptomyces hygroscopicus, Food Chem. 105 (2007), https://doi.org/10.1016/j.foodchem.2007.04.020.
[32] M.L. Ho, S.Z. Leu, J.F. Hsieh, S.T. Jiang, Technical approach to simplify the purification method and characterization of microbial transglutaminase produced from *Streptoverticillium ladakanum*, J. Food Sci. 65 (2000), https://doi.org/10.1111/j.1365-2621.2000.tb15959.x.
[33] S.M.T. Gharibzahedi, I.S. Chronakis, Crosslinking of milk proteins by microbial transglutaminase: utilization in functional yogurt products, Food Chem. 245 (2018), https://doi.org/10.1016/j.foodchem.2017.10.138.
[34] B. García-Gómez, M.L. Vázquez-Odériz, N. Muñoz-Ferreiro, M.A. Romero-Rodríguez, M. Vázquez, Effect of the milk heat treatment on properties of low-fat yogurt manufactured with microbial transglutaminase, Emir. J. Food Agric. 32 (2020), https://doi.org/10.9755/ejfa.2020.v32.i10.2180.
[35] E.A. Romeih, M. Abdel-Hamid, A.A. Awad, The addition of buttermilk powder and transglutaminase improves textural and organoleptic properties of fat-free buffalo yogurt, Dairy Sci. Technol. 94 (2014), https://doi.org/10.1007/s13594-014-0163-8.
[36] A. Gilbert, L.E. Rioux, D. St-Gelais, S.L. Turgeon, Characterization of syneresis phenomena in stirred acid milk gel using low frequency nuclear magnetic resonance on hydrogen and image analyses, Food Hydrocoll. 106 (2020), https://doi.org/10.1016/j.foodhyd.2020.105907.
[37] F. Koohzad, A. Asoodeh, Cross-linked electrospun pH-sensitive nanofibers adsorbed with Temporin-Ra for promoting wound healing, ACS Appl. Mater. Interfaces 15 (2023), https://doi.org/10.1021/acsami.2c23268.
[38] F. Coccolini, R. Coimbra, C. Ordonez, Y. Kluger, F. Vega, E.E. Moore, W. Biffl, A. Peitzman, T. Horer, F.M. Abu-Zidan, M. Sartelli, G.P. Fraga, E. Cicuttin, L. Ansaloni, M.W. Parra, M. Millán, N. Deangelis, K. Inaba, G. Velmahos, R. Maier, V. Khokha, B. Sakakushev, G. Augustin, S. Di Saverio, E. Pikoulis, M. Chirica, V. Reva, A. Leppaniemi, V. Manchev, M. Chiarugi, D. Damaskos, D. Weber, N. Parry, Z. Demetrashvili, I. Civil, L. Napolitano, D. Corbella, F. Catena, H. Bahouth, M. Tolonen, P. Fugazzola, J.J. Serna, F. Rodriguez, A.F. Garciá, A. Gonzalez, L.F. Pino, M. Guzmán-Rodríguez, B.M. Pereira, A. Kirkpatrick, A.C. Mefire, A. Tarasconi, O. Chiara, C.A. Gomes, J. Galante, M. Bala, P. Perfetti, F. MacHado, O. Romeo, F. Salvetti, L. Ghiadoni, F. Forfori, P. Malacarne, S. Pini, M. Pucciarelli, M. Ceresoli, C. Arvieux, D. Khokha, D.A. Spain, A. Isik, Liver trauma: WSES 2020 guidelines, World J. Emerg. Surg. 15 (2020), https://doi.org/10.1186/s13017-020-00302-7.
[39] S.Y.N. Kumari, S. Kadiri, Optimization of antimicrobial metabolites production by Streptomyces fradiae, Int, J. Pharm. Pharm. Sci. 2 (2015).
[40] C. Bourneow, S. Benjakul, P. Sumpavapol, A. H-Kittikun, Isolation and cultivation of transglutaminase producing bacteria from seafood processing factories, Innov rom, Food Biotechnol. 10 (2012).
[41] Y.N. Fawzya, Microbial transglutaminase of Indonesian Streptomyces sp.: screening and production in several media, Squalen Bulletin of Marine and Fisheries Postharvest and Biotechnology 11 (2016), https://doi.org/10.15578/squalen.v11i1.195.
[42] S. Khunthongpan, A. H-Kittikun, C. Bourneow, S. Tanasupawat, P. Sumpavapol, Identification of Transglutaminase-Producing Bacterium Isolated from Seafood Processing Wastewater, n.d.
[43] K. Yokoyama, N. Nio, Y. Kikuchi, Properties and applications of microbial transglutaminase, Appl. Microbiol. Biotechnol. 64 (2004), https://doi.org/10.1007/s00253-003-1539-5.

[44] S.Y. Lu, N.D. Zhou, Y.P. Tian, H.Z. Li, J. Chen, Purification and properties of transglutaminase from Streptoverticillium mobaraense, J. Food Biochem. 27 (2003), https://doi.org/10.1111/j.1745-4514.2003.tb00270.x.
[45] A. Duerasch, J. Wissel, T. Henle, Reassembling of alkali-treated casein micelles by microbial transglutaminase, J. Agric. Food Chem. 66 (2018), https://doi.org/10.1021/acs.jafc.8b04000.
[46] M. Kieliszek, A. Misiewicz, Microbial transglutaminase and its application in the food industry. A review, Folia Microbiol. (Praha) 59 (2014), https://doi.org/10.1007/s12223-013-0287-x.
[47] Y. Zhu, A. Rinzema, J. Tramper, J. Bol, Medium design based on stoichiometric analysis of microbial transglutaminase production by Streptoverticillium mobaraense, Biotechnol. Bioeng. 50 (1996), https://doi.org/10.1002/(SICI)1097-0290(19960505)50:3<291::AID-BIT8>3.0.CO;2-B.
[48] M. Griffin, R. Casadio, C.M. Bergamini, Transglutaminases: Nature's biological glues, Biochem. J. 368 (2002), https://doi.org/10.1042/BJ20021234.
[49] T.A.E. Ahmed, E.V. Dare, M. Hincke, Fibrin: a versatile scaffold for tissue engineering applications, Tissue Eng. Part B Rev. 14 (2008), https://doi.org/10.1089/ten.teb.2007.0435.